C.P. No. 1237

C.P. No. 1237

MINISTRY OF DEFENCE (PROCUREMENT EXECUTIVE)

AERONAUTICAL RESEARCH COUNCIL

CURRENT PAPERS

On the Effects of Viscous Interaction for a Flat Delta Wing at Incidence

By

L. Davies

Aerodynamics Division, NPL

LONDON· HER MAJESTY'S STATIONERY OFFICE

1973

Price 55p net

CP No. 1237*
May, 1970

ON THE EFFECTS OF VISCOUS INTERACTION FOR A FLAT DELTA WING AT INCIDENCE

by

L. Davies
Aerodynamics Division, NPL

SUMMARY

The pressures induced on the surface of a flat delta wing as a result of the interaction of the viscous layer with the external flow can result in large increases in the normal force. Equations are derived in this paper which allow the magnitude of these increases to be assessed.

List of Contents

Part II./

---

*Replaces A.R.C.32 117

Page

Part II. General Two-Dimensional Second-Order Theory

Nomenclature/

Nomenclature

A	area
A_R	reference area
a	constant
b	constant
C	Chapman-Rubesin Factor $\left(= \frac{\mu_w}{\mu_\infty} \cdot \frac{T_\infty}{T_w}\right)$ where μ is fluid viscosity and subscripts '∞' and 'w' refer to free-stream and wall conditions
C_N	normal-force coefficient
$\overline{C}_N$	total normal-force coefficient, including components due to both strong- and weak-interaction effects, and also the inviscid flow
$C_{N,i}$	inviscid normal-force coefficient
$C_{N,w}$	weak-interaction region normal-force coefficient
$C_{N,s}$	strong-interaction region normal-force coefficient
$C^*_{N,w}$	weak-interaction plus inviscid normal-force coefficient
$C^*_{N,s}$	strong-interaction plus inviscid normal-force coefficient
$\overline{C}_{N,IN}$	insulated-wall total normal-force coefficient
$C_{N,m}$	merged-region normal-force coefficient
C_p	pressure coefficient
$C_{p,w}, C_{p,s}$	local, total pressure coefficients in weak- and strong-interaction regions respectively
L	chord length
ℓ	half base width of delta
M_b	oblique shock inviscid Mach number for plate at incidence
M_∞	free-stream Mach number
p_b	inviscid pressure behind oblique shock
p_∞	free-stream pressure

Re_∞/

Re_∞	free-stream Reynolds number
Re_u	unit Reynolds number over delta surface based on inviscid conditions outside the viscous layer
T_w	wall temperature
T_∞	free-stream temperature
T_o	reservoir temperature
$\bar{V}_\infty$	interaction parameter = $M_\infty \sqrt{C}/\sqrt{Re_\infty}$
x_1, x_2	lengths defined in Fig. 1
$X_{C.P.}$	distance of centre-of-pressure from base
α	angle of incidence
β	oblique shock angle
γ	ratio of specific heats
λ	expression used in Section 6, (Part II)
$\zeta_i(\alpha)$	function of α defined in equation (21), (Part I)
$\psi_i(\alpha)$	" " " " " " (4), (Part II)
$\xi_i(\alpha)$	" " " " " " (8) and (12), (Part I) and equation (4), (Part II)
ϕ	sweep-back angle for delta wing
$\bar{\chi}$	viscous-interaction parameter, $M^3\sqrt{C}/\sqrt{Re}$
$\bar{\chi}_u$	$\bar{\chi}$, based on Re_u, M_b
$\bar{\chi}_\infty$	$\bar{\chi}$, based on Re_∞, M_∞

Introduction/

Introduction

As a result of the great activity during the last decade in the field of low-density aerodynamics, stimulated largely by the problems of spacecraft re-entry, there is a wealth of information on the viscous-induced pressure distributions for simple geometric shapes. These data can usually be represented by equations of first or second order in terms of a viscous-interaction correlation parameter $\bar{\chi}$ which will be described later, and the values of the constants in these equations and the validity of the second-order terms are the subject of much discussion.

Without entering into such a discussion (which is beyond the terms of reference of the present paper) we shall take some examples of likely first- and second-order equations in order to illustrate the effects of viscous interaction on the normal force acting on a flat delta wing.

These effects can be significant for the moderate Reynolds numbers and hypersonic Mach numbers frequently encountered in test facilities, and in order that meaningful analyses may be made it is necessary that the magnitude and range of applicability of the viscous-interaction corrections to the aerodynamic forces be determined. This is the purpose of the present paper.

The paper is divided into two sections. In the first a simple theory is used to develop first-order expressions only, and in the second a more general* two-dimensional second-order theory is presented.

Part I/

---

* The term 'general' used in this context merely implies that the equations are in a form into which any first- or second-order correlating theory may be substituted. It does not imply any completeness; on the contrary this is still an elementary two-dimensional strip-theory approach.

Part I. Simple Two-Dimensional First-Order Theory

1. Effects of Viscosity

The pressure distribution on a flat plate at zero incidence in a hypersonic flow at moderate or low Reynolds number can be very different from the value assumed for the inviscid flow. The extent of the departure depends on the Mach number and Reynolds number. The flow near the leading edge is very complex, particularly if the density is low enough for free molecular flow to be present, but for our present purposes let it suffice that at the leading edge the shock and boundary layer merge, and that this is followed by a 'strong-interaction region' where the boundary layer grows roughly as $x^{3/4}$. Here the streamline inclinations produced in the external flow are large and the pressure and viscous terms have about the same magnitude[1]. Further downstream, where the boundary-layer growth is proportional to $x^{1/2}$, there is the 'weak-interaction régime' which extends far downstream. Here the effects produced by the boundary layer on the external flow are mainly perturbations on the existing uniform flow. The regions where the various régimes join depend on the flow Mach number, Reynolds number and the temperature of the plate surface.

A viscous-interaction correlation parameter $\bar{\chi}_\infty$ can be used to describe these various regions of the flow, where

$$\bar{\chi}_\infty = M_\infty^3 \sqrt{C_\infty} / \sqrt{Re_\infty} \qquad \cdots (1)$$

Here C is the Chapman-Rubesin factor relating temperature and viscosity. For a 'cold-wall' plate where the surface temperature is a small fraction of the reservoir temperature, the boundary between the strong- and weak-interaction regions occurs typically at a value $\bar{\chi} \approx 10$, whereas for an 'insulated-plate' surface, where the surface temperature approaches that of the reservoir, the appropriate value is $\bar{\chi} \approx 3{\cdot}5$. A further correlation parameter $\bar{V}$ is more relevant in the region where there is merging between the shock and the boundary layer, and

$$\bar{V}_\infty = M_\infty \sqrt{C_\infty} / \sqrt{Re_\infty} = \frac{\bar{\chi}_\infty}{M_\infty^2} \qquad \cdots (2)$$

Metcalf et al[2], amongst others, have shown that merging occurs, over a wide range of Mach numbers, for values of $\bar{V}$ in the range $0{\cdot}15 \leqslant V \leqslant 0{\cdot}2$.

The surface pressure distributions on the plate differ for the cold- and insulated-wall conditions, and so whilst determining the effects of boundary-layer growth for the present series of tests where cold-wall conditions apply, we have also derived the conditions appropriate to the insulated-wall case.

The effects of viscosity briefly introduced above will be examined in detail, as they apply to the flat delta wing, in the next section.

2./

2. The Effects of Viscosity on the Flow over a Flat Delta Wing

Cooke[3] has suggested that for the inviscid-flow design criteria to be met the greatest allowable value of $\bar{\chi}$ at the maximum chord length of a caret wing should not exceed 0·22. For values less than this no more than 5% of the wing area would be affected significantly by viscous interaction. Instead of following Cooke's approach we will derive analytical expressions for the forces acting as a result of viscous interaction for both the cold and insulated wall cases, using a modified form of strip theory. In this method we take strips parallel to the leading edge, instead of the centre chord, so that the value of $\bar{\chi}$ remains constant along any strip. At incidence (α) we assume that the boundary layer on a strip grows as a function of the local inviscid-flow conditions predicted by oblique-shock theory or Prandtl-Meyer expansion.

The pressure distributions over the flat plate are given in terms of $\bar{\chi}$ by expressions of the form

$$p(\bar{\chi}) = p_b + p_b\, a\, \bar{\chi} \ldots \quad \text{first-order weak interaction} \quad \cdots (3)$$

and

$$p(\bar{\chi}) = p_b\, b\, \bar{\chi} \ldots \quad \text{first-order strong interaction} \quad \cdots (4)$$

where p_b is the appropriate local static pressure for inviscid flow (note that at zero incidence $p_b = p_\infty$).

Here $\bar{\chi}$ is referred to conditions outside the viscous layer. The values of the constants a and b will depend on wall temperature. A number of values of a and b have been derived and are quoted in the literature, and some of these have been collected and discussed in Refs. 4 and 5.

The method of solution in the present paper will be discussed with reference to Fig. 1. The area of an elementary strip is $x \tan \phi\, dx$ and the forces acting on this strip will depend on the particular pressure-distribution equation used. We assume that the weak-interaction régime exists up to a distance x_1 which is calculated using the appropriate value of $\bar{\chi}$ for the junction criterion. Strong-interaction theory is then used from x_1 up to x_2, where merging is assumed to terminate the integration, and x_2 has been computed using $\bar{V} = 0{\cdot}2$. In fact, x_2 is so near the leading edge for our calculations that we have assumed, with little loss in accuracy, that strong-interaction theory can be used right up to the leading edge. This allows for some simplification as will be demonstrated. However, the full equations are included for use at low Reynolds numbers. What happens when there is an appreciable merged region, a situation produced in a recent experiment by Metcalf et al for example, is a little beyond the terms of reference of the present paper but some tentative suggestions are made briefly in a later section.

The force coefficient acting normal to the compression surface of the delta can therefore be represented by an equation of the form

$$\bar{C}_N = C^*_{N,w} + C^*_{N,s} \quad \cdots (5)$$

where/

where $\bar{C}_N$ is the total force on this surface formed by the sum of the normal-force contributions in the weak-interaction and strong-interaction regions ($C^*_{N,w}$ and $C^*_{N,s}$ respectively). Using the first-order pressure-distribution equation we have for the weak-interaction régime

$$C_{p,w}(\bar{\chi}) = \frac{(p(\bar{\chi})-p_\infty)}{p_\infty} \cdot \frac{2}{\gamma M_\infty^2} = \frac{(p_b+p_b\, a\bar{\chi}-p_\infty)}{p_\infty} \cdot \frac{2}{\gamma M_\infty^2} = C_{p,i} + a\left(\frac{p_b}{p_\infty}\right) \frac{\bar{\chi}2}{\gamma M_\infty^2} \qquad \cdots (6)$$

where $C_{p,w}$ is the total local pressure coefficient in the weak-interaction region, and $C_{p,i}$ is the component due to inviscid pressure. The sum of the forces acting on the surface for the weak-interaction region is therefore

$$C^*_{N,w} = 2\int_0^{x_1} \left(C_{p,i} + a\left(\frac{p_b}{p_\infty}\right) \frac{2}{\gamma M_\infty^2}\, \bar{\chi}\right) \frac{x \tan \phi}{A_R}\, dx. \qquad \cdots (7)$$

$$= C_{N,i} \int_0^{x_1} + \frac{4a}{\gamma M_\infty^2} \left(\frac{p_b}{p_\infty}\right) \frac{M_b^3}{\sqrt{Re_u}} \frac{\tan^{\frac{1}{2}}\phi}{A_R} \int_0^{x_1} \frac{x}{\sqrt{\ell - x}}\, dx$$

$$= C_{N,i} \int_0^{x_1} + \xi_1(\alpha) \int_0^{x_1} \frac{x}{\sqrt{\ell - x}}\, dx \qquad \cdots (8)$$

where $\xi_1(\alpha)$ is a constant for fixed α. Note that we assume $\sqrt{C_b} = 1$.

In the strong-interaction region

$$C_{p,s} = \left(\frac{b\bar{\chi}\ p_b - p_\infty}{p_\infty}\right) \frac{2}{\gamma M_\infty^2} = \left(\frac{b\bar{\chi}\ p_b + p_b - p_b - p_\infty}{p_\infty}\right) \frac{2}{\gamma M_\infty^2}$$

$$= C_{p,i} + \frac{p_b}{p_\infty} \cdot (b\bar{\chi}-1) \frac{2}{\gamma M_\infty^2} \qquad \cdots (9)$$

and the force contributed by this region to the surface is given by

$C^*_{N,s}$/

$$C^*_{N,s} = 2\int_{x_1}^{x_2} \left(C_{p,i} + \frac{p_b}{p_\infty}\left(b\bar{\gamma} - 1\right) \frac{2}{\gamma M_\infty^2} \right) \frac{x \tan \phi}{A_R}\, dx \qquad \cdots (10)$$

$$= C_{N,i} \Big|_{x_1}^{x_2} + \xi_2(\alpha) \int_{x_1}^{x_2} \frac{x}{\sqrt{\ell - x}}\, dx - \xi_3(\alpha) \int_{x}^{x_2} 2x\, dx \qquad \cdots (11)$$

where

$$\xi_2(\alpha) = \frac{4b}{\gamma M_\infty^2}\left(\frac{p_b}{p_\infty}\right) \frac{\tan^{\frac{1}{2}}\phi}{A_R} \cdot \frac{M_b^3}{\sqrt{Re_u}}, \quad \text{and} \quad \xi_3(\alpha) = \frac{2}{\gamma M_\infty^2} \frac{\tan \phi}{A_R}\left(\frac{p_b}{p_\infty}\right)$$

$$\cdots (12)$$

Equation (5) can now be modified to

$$\tilde{C}_N = C^*_{N,w} + C^*_{N,s} = C_{N,i} + C_{N,w} + C_{N,s} \qquad \cdots (13)$$

where $C^*_{N,w}$ and $C^*_{N,s}$ are the appropriate viscous terms from equations (8) and (11) and $C_{N,w}$ and $C_{N,s}$ are now the incremental normal-force coefficients induced by weak- and strong-interaction effects respectively. The effects of viscosity can therefore be conveniently represented as a perturbation on the force coefficient for inviscid flow.

Equation (13) is the general expression for viscous interaction if the limit x_2 is allowed to go to the leading edge, and the cold- or insulated-wall cases can be obtained by inserting the appropriate values for a and b, and for the integration limits.

3. Insulated Wall

For the constants a and b we have chosen those quoted by Cox and Crabtree[6], and x_1 has been determined using $\bar{\gamma} = 3{\cdot}5$. It is assumed that $x_2 = \ell$ (see Fig. 1). The expression for the normal force for an insulated-wall plate is therefore

$$\bar{C}_{N,IN} = C_{N,i} + \frac{2}{3}\xi_1(\alpha)\left\{\left(\frac{b}{a} - 1\right)\left(\sqrt{\ell - x_1}\,(x_1 + 2\ell)\right) + 2\ell^{\frac{3}{2}}\right\}$$

$$- \xi_3(\alpha)\,(\ell^2 - x_1^2) \qquad \cdots (14)$$

4. Cold Wall

In this case we have again chosen values of a and b from Cox and Crabtree, and since the value of $\bar{\gamma}$ for the overlap region gives a value of x_1 which is very close to x_2, and similarly since x_2

is/

is approximately equal to ℓ, we have assumed that $x_1 = x_2 = \ell$. Consequently there is no strong-interaction contribution to the normal force, and equation (13) has the following simple form

$$\bar{C}_N = C_{N,i} + \frac{2}{3}\xi_1(\alpha)\ell^{\frac{3}{2}} \qquad \cdots(15)$$

5. Comparison of Forces in Inviscid and Viscous Flow

The insulated- and cold-wall force coefficients normal to the lower or pressure surface of a 76° swept delta for the NPL shock-tunnel conditions and for the incidence range $0° \leqslant \alpha \leqslant 20°$ have been plotted in Fig. 2. The two viscous-flow cases are compared with the curve for inviscid flow using two-dimensional strip theory, and in Fig. 3 the percentage increases in normal force for the two viscous-flow cases are indicated. It is evident that relatively large departures from the inviscid-flow values of normal force will occur as a result of viscous interaction, and that the increase for the insulated-wall case is some two or three times the cold-wall values. The consequences of this conclusion will be significant for continuously-running facilities and for actual cruising flight conditions where the insulated-wall conditions may sometimes apply.

6. Movement of the Centre-of-Pressure

The position of the centre-of-pressure for a flat delta in inviscid flow is along the centre line a distance of 2/3 chord from the apex. However, when viscous-interaction effects are significant the centre-of-pressure will lie closer to the apex because of the higher pressures produced near the leading edge.

The general expression for the centre-of-pressure distance from the trailing edge of the delta, including the effects of viscous interaction, is

$$X_{C.P.}\left(1 + \frac{\bar{C}_N - C_{N,i}}{C_{N,i}}\right) = \frac{L}{3} + \frac{\xi_1'(\alpha)}{C_{N,i}}\left\{\left(\frac{b}{a} - 1\right)\left(2\ell^2\sqrt{\ell - x_1} - \frac{4}{3}\ell(\ell - x_1)^{\frac{3}{2}} + \right.\right.$$

$$\left.\left. + \frac{2}{5}(\ell - x_1)^{\frac{5}{2}}\right) + \frac{16}{15}\ell^{\frac{5}{2}}\right\}$$

$$- \frac{\xi_1'(\alpha)}{C_{N,i}}\,\frac{b}{a}\left(2\ell^2\sqrt{\ell - x_2} - \frac{4}{3}\ell(\ell - x_1)^{\frac{3}{2}} + \frac{2}{5}(\ell - x_1)^{\frac{5}{2}}\right)$$

$$- \frac{\xi_2'(\alpha)}{3}(x_2^3 - x_1^3) \qquad \cdots (16)$$

(where/

(where $\xi_i'(\alpha) = \xi_i(\alpha) \tan \phi/2$)

$$= \frac{L}{3} + \frac{\xi'(\alpha)}{C_{N,i}} \left\{ \left(\frac{b}{a} - 1 \right) f(x_1, \ell) + \frac{16}{15} \ell^{\frac{5}{2}} \right\} -$$

$$- \frac{\xi_1(\alpha)}{C_{N,i}} \frac{b}{a} f(x_2, \ell) - \frac{\xi_3'(\alpha)}{3} (x_1^3 - x_2^3) \qquad \cdots (17)$$

Here L is the centre chord length.

For the insulated-wall case if we assume that $x_2 = \ell$ then

$$f(x_1, \ell) = 0 \ ;$$

for the cold-wall case we assume that $x_1 = x_2 = \ell$ and so

$$f(x_2, \ell) = f(x_1, \ell) = 0 \ ;$$

therefore equation (17) reduces to the simple expression

$$X_{C.P.} = \left(\frac{L}{3} + \frac{\xi'(\alpha)}{C_{N,i}} \frac{16}{15} \ell^{\frac{5}{2}} \right) \cdot \left(1 + \frac{\bar{C}_N - C_{N,i}}{C_{N,i}} \right)^{-1} \qquad \cdots (18)$$

The centre-of-pressure positions for the three cases (inviscid flow, insulated wall and cold wall respectively), have been plotted as functions of incidence in Fig. 4. As in the normal-force comparison we find that the largest effect occurs with an insulated wall. In Fig. 4 the continuous curves are those obtained using the above theory, whereas the broken curves have been computed by using $\left(\frac{M_\infty}{M_b} \right) \cdot \bar{\chi}$ instead of $\bar{\chi}$ in the pressure functions. This point is discussed further in Section 8.

7. Rectangular Flat Plate at Incidence

In the rectangular flat-plate case we take strips again parallel to the leading edge, as we did for the delta, but now the problem is of course much simpler. The details of the calculations are very similar to those for the delta and will therefore not be repeated. For the insulated-wall case the normal-force equation has the form

$$\bar{C}_N = C_{N,1} + \frac{1}{2} \left\{ x_1^{\frac{1}{2}} (\zeta_1(\alpha) - \zeta_2(\alpha)) + \zeta_2(\alpha) x^{\frac{1}{2}} \right\} - \zeta_3(\alpha)(x_2 - x_1)$$

$$\cdots (19)$$

For/

For the cold-wall case the equation is

$$\bar{C}_N = C_{N,i} + \frac{\zeta_1(\alpha)}{2} \ell^{\frac{1}{2}} \qquad \cdots (20)$$

Here ℓ is the plate length in the streamwise direction, and W its width

where
$$\left.\begin{aligned} \zeta_1(\alpha) &= \frac{2aW}{\gamma M_\infty^2}\left(\frac{p_b}{p_\infty}\right)\frac{M_b^3}{\sqrt{Re_u}}\,\frac{1}{A_R} \\ \zeta_2(\alpha) &= \frac{2bW}{\gamma M_\infty^2}\left(\frac{p_b}{p_\infty}\right)\frac{M_b^3}{\sqrt{Re_u}}\cdot\frac{1}{A_R} = \zeta_1(\alpha)\,\frac{b}{a} \\ \zeta_3(\alpha) &= \frac{2W}{\gamma M_\infty^2}\left(\frac{p_b}{p_\infty}\right) \end{aligned}\right\} \qquad \cdots (21)$$

As in the case of the delta wing the centre-of-pressure lies nearer the leading edge for the viscous case than when the flow is assumed inviscid.

8. Discussion

The effects of viscous interaction on the normal force for the pressure (lower) surface of a flat delta are seen from Figs. 2 and 3 to be quite large even for moderately high Reynolds numbers. In the present calculations the Reynolds number based on chord length was $0{\cdot}45 \times 10^6$, and the Mach number was 8·6; for these conditions increases of over 50% in lower-surface normal force are to be expected for incidences less than 5° when insulated-wall conditions apply, and increases of over 15% are obtained for the cold-wall cases. These percentages shown by the full curves in Figs. 2, 3 and 4 are probably underestimates due to the use of the pressure distribution derived assuming that the boundary layer grows as a function of the oblique-shock conditions of inviscid flow. Metcalf has suggested, from correlations of flat-plate pressures at incidence, that a weighting factor (M_∞/M_b) should be used[5] so that the coefficient of $\bar{\chi}$ is the product of the oblique-shock value times the weighting factor. If we do this then we obtain the broken curves in Figs. 2, 3 and 4, which indicate a significant increase in the predicted effects of viscous interaction.

The combination of increased normal force and forward movement of the centre-of-pressure will result in a large increase in pitching moment about the base. Clearly then it is the pitching moment which will be most affected by viscous interaction. For example a 5% increase in normal force, together with a 5% forward movement of the centre-of-pressure, will produce a 10% increase in pitching moment about the base line of the delta wing.

The/

The effects of decreasing Reynolds number on total normal force for the lower surface are indicated in Fig. 5, where the results consequent upon an order of magnitude decrease in Reynolds number are illustrated. There is almost 100% increase in $\bar{C}_N$ for the insulated-wall case for incidences less than 5°, and the cold-wall values have increased by about half this amount.

As regards the upper, or expansion, surface of the delta wing, the local Mach number increases considerably with incidence and there is a large fall in local Reynolds number. This combination leads to a large increase in $\bar{\chi}$ and hence considerable viscous interaction effects. However as can be seen from Figs. 6 and 7 (where the total inviscid-flow and viscous-flow normal forces for this surface and their percentage differences are plotted respectively), the change in normal force is not as dramatic as may have been expected. The reason for this is that although a considerable pressure perturbation is produced, the expression $(1 - p_b/p_\infty)$ tends to unity as incidence increases and so even an increase of two or three times the inviscid pressure will not result in a large change in the absolute level of the surface pressure coefficient, or of course to the magnitude of the upper surfaces contribution to the wing normal force.

The conclusion is therefore that except for the zero incidence case, and for very small incidence, where the upper and lower normal force coefficients are comparable (for the infinitely thin delta wing) it is the lower, or pressure, surface force increment which is dominant.

In Part II the general, two-dimensional equations for viscous normal force are derived and it will be seen that the results are in many ways similar to those described above.

Part II./

Part II. General Two-Dimensional Second-Order Theory

In this section the general equations for the effects of viscosity on the flow over a flat delta wing at hypersonic speeds will be derived. The approach is very similar to that described in Part I, and hence only the outline of the theory will be given.

1. Weak-Interaction Régime

The pressure on the surface of a strip in Fig. 1 will now be represented as an equation of second order in $\bar{\chi}$, as follows

$$\frac{p}{p_b} = a_0 + a_1 \bar{\chi} + a_2 \bar{\chi}^2 = \sum_{n=0}^{2} a_n \bar{\chi}^n \qquad \cdots (1)$$

The total normal force on the surface in the weak-interaction region is therefore

$$\bar{C}_{N,w} = 2 \int_0^{x_1} \left(\frac{p_b}{p_\infty} \sum_{n=0}^{2} a_n \bar{\chi}^n - 1 \right) \frac{2}{\gamma M_\infty^2} \cdot \frac{x \tan \phi}{A_R} \, dx \qquad \cdots (2)$$

and on integrating we have

$$= C_{N,i} \Big|_0^{x_1} + \psi_1(\alpha)\, x_1^2 + \frac{2}{3} \psi_2(\alpha) \left[2\ell^{\frac{3}{2}} - \sqrt{\ell - x_1}\,(x_1 + 2\ell) \right] +$$

$$+ \psi_3(\alpha) \left[\log_e e^{\ell} - (x_1 + \log_e (\ell - x_1)^{\ell}) \right] \qquad \cdots (3)$$

where

$$\left.\begin{aligned} \psi_1(\alpha) &= (a_0 - 1) \frac{p_b}{p_\infty} \cdot \frac{2}{\gamma M_\infty^2} \cdot \frac{\tan \phi}{A_R} \\ \psi_2(\alpha) &= \frac{4a_1}{\gamma M_\infty^2} \cdot \frac{p_b}{p_\infty} \cdot \frac{M_b^2}{\sqrt{Re_u}} \cdot \frac{\tan^{\frac{1}{2}} \phi}{A_R} \\ \psi_3(\alpha) &= \frac{4a_2}{\gamma M_\infty^2} \cdot \frac{p_b}{p_\infty} \cdot \frac{M_b^6}{Re_u} \cdot \frac{1}{A_R} \end{aligned}\right\} \qquad \cdots (4)$$

For/

For the cold-wall case, if we let $x_1 = \ell$ everywhere except in the expression $\log_e(\ell - x_1)$, then

$$\left(\bar{C}_N\right)_{\frac{T_w}{T_o}\to 0} = C_{N,i} + \psi_1(\alpha)\ell^2 + \frac{4}{3}\psi_2(\alpha)\ell^{\frac{3}{2}} + \psi_3(\alpha)\log_e\left(\frac{\ell}{\ell - x_1}\right)^{\ell} \quad \cdots (5)$$

and for general first-order theory $\left(\frac{p}{p_b} = a_o + a_1\bar{\chi}\right)$, where $\psi_3(\alpha) = 0$ then

$$\left(\bar{C}_N\right)_{\frac{T_w}{T_o}\to 0} = C_{N,i} + \psi_1(\alpha)\ell^2 + \frac{4}{3}\psi_2(\alpha)\ell^{\frac{3}{2}} \quad \cdots (6)$$

2. Strong Interaction

The total normal force on the surface in the strong-interaction region is

$$\bar{C}_{N,s} = 2\int_{x_1}^{x_2}\left(\frac{p_b}{p_\infty}\sum_{n=0}^{2} b_n\bar{\chi}^n - 1\right)\frac{2}{\gamma M_\infty^2}\cdot\frac{x\tan\phi}{A_R}\,dx \quad \cdots (7)$$

where

$$\sum_{n=0}^{2} b_n\bar{\chi}^n = b_o + b_1\bar{\chi} + b_2\bar{\chi}^2.$$

On integrating we have

$$\bar{C}_{N,s} = C_{N,1}\Big|_{x_1}^{x_2} + \frac{(b_o - 1)}{(a_o - 1)}\psi_1(\alpha)(x_2^2 - x_1^2) + \frac{2}{3}\frac{b_1}{a_1}\psi_2(\alpha)\times$$

$$\times\left[\sqrt{\ell - x_1}(x_1 + 2\ell) - \sqrt{\ell - x_2}\,(x_2 + 2\ell)\right] +$$

$$+\frac{b_2}{a_2}\psi_3(\alpha)\left[x_1 - x_2 + \log_e\left(\frac{\ell - x_1}{\ell - x_2}\right)^{\ell}\right] \quad \cdots (8)$$

Most/

Most weak-interaction pressure distributions are represented in terms of $\bar{\chi}$ as shown in equation (2). However the strong-interaction region pressure distribution is not always a function of increasing powers of $\bar{\chi}$. If we therefore assign the function $f(n)$ as the power to which $\bar{\chi}$ is raised, where $f(n)$ is any simple function of n, e.g. $(1 - n)$ (Ref.6), then

$$\frac{p}{p_b} = b_n \bar{\chi}^{f(n)}$$

and it is readily shown that in this case

$$\bar{C}_{N,s} = \lambda_1 \left\{ \left[\sum_{n=0}^{m} b_n^* \left\{ \frac{-x}{(\ell - x)^{(f(n)-1)}(2 - f(n))} - \frac{\ell(\ell - x)^{(1-f(n))}}{(2 - f(n))} \right\} \right]_{x_1}^{x_2} - \frac{(x_2^2 - x_1^2)}{2} \right\}$$

where $$\lambda_1 = 4 \frac{p_b}{p_\infty} \cdot \frac{1}{\gamma M_\infty} \cdot \frac{\tan \phi}{A_R}$$

and $$b_n^* = b_n \left(\frac{M_b^3}{\sqrt{Re_u}} \cdot \left(\frac{M_\infty}{M_b} \right) \right)^{f(n)}$$

For the computations in the present paper, however, the form given in equation (8) will be used exclusively.

3. Total Force

If we now combine the contributions to the total force from the weak- and the strong-interaction regions, we have

$\bar{C}_N$ /

$$\bar{C}_N = C_{N,i} + \psi_1(\alpha)\left[x_1^2 + \frac{(b_o - 1)}{(a_o - 1)}(x_2^2 - x_1^2)\right] + \frac{2}{3}\psi_2(\alpha)\left[2\ell^{\frac{3}{2}} - \right.$$

$$\left. - \frac{b_1}{b_2}\sqrt{\ell - x_2}\,(x_2 + 2\ell) + \left(\frac{b_1}{a_1} - 1\right)\sqrt{\ell - x_1}\,(x_1 + 2\ell)\right] +$$

$$+ \psi_3(\alpha)\left[\left(\frac{b_2}{a_2} - 1\right)x_1 + \log_e\left\{\left(\frac{\ell}{\ell - x_1}\right)^{\ell}\cdot\left(\frac{\ell - x_1}{\ell - x_2}\right)^{\varepsilon}\right\}\right] \quad \cdots (9)$$

where

$$\varepsilon = \frac{b_2 \ell}{a_2}$$

4. Centre-of-Pressure Position

The moment of the weak-interaction region force about the base line is

$$X_w \bar{C}_{N,w} = C_{p,i}\frac{\tan\phi}{A_R}\frac{x_1^3}{6} + \psi_1(\alpha)\tan\phi\frac{x_1^3}{3} + \psi_2(\alpha)\frac{\tan\phi}{2} \times$$

$$\times \left[-2\ell^2\sqrt{\ell - x_1} + \frac{4}{3}\ell(\ell - x_1)^{\frac{3}{2}} - \frac{2}{5}(\ell - x_1)^{\frac{5}{2}} + \frac{16}{15}\ell^{\frac{5}{2}}\right] +$$

$$+ \psi_3(\alpha)\frac{\tan\phi}{2}\left[\log_e\left(\frac{\ell}{\ell - x_1}\right)^{\ell^2} - \frac{x_1(2\ell + x_1)}{2}\right] \quad \cdots (10)$$

and for the strong-interaction region

$X_s \bar{C}_{N,s}$/

$$X_s \bar{C}_{N,s} = C_{p,i} \frac{\tan \phi}{6 A_R} (x_2^3 - x_1^3) + \frac{(b_o - 1)}{(a_o - 1)} \frac{\psi_1(\alpha) \tan \phi}{3} (x_2^3 - x_1^3) +$$

$$+ \frac{b_1}{a_1} \psi_2(\alpha) \frac{\tan \phi}{2} \left[- 2\ell^2 \sqrt{\ell - x_2} + \frac{4}{3} \ell (\ell - x_2)^{\frac{3}{2}} - \frac{2}{5} (\ell - x_2)^{\frac{5}{2}} + \right.$$

$$\left. + 2\ell^2 \sqrt{\ell - x_1} - \frac{4}{3} \ell (\ell - x_1)^{\frac{3}{2}} + \frac{2}{5} (\ell - x_1)^{\frac{5}{2}} \right] +$$

$$+ \frac{b_2}{a_2} \psi_3(\alpha) \frac{\tan \phi}{2} \left[\frac{x_1^2}{2} - \frac{x_2^2}{2} + \ell (x_1 - x_2) + \right.$$

$$\left. + \log_e \left(\frac{\ell - x_1}{\ell - x_2} \right)^{\ell^2} \right] \qquad \cdots (11)$$

The centre-of-pressure position is then found from

$$X_{C.P.} \cdot \bar{C}_N = (X_w C_{N,w} + X_s C_{N,s}) \qquad \cdots (12)$$

The normal-force predictions for various available theories for viscous-interaction effects are plotted in Fig. 8.

5. Merged-Region Force Coefficient

The form of the pressure distribution in this region is not at all well known, because of the difficulty in making measurements very close to the leading edge. Any guess at the form of the distribution must necessarily be tentative in the extreme. However, it is observed that when merging occurs the pressure reaches a plateau and subsequently falls to about the free-stream value at the leading edge. As a first guess a trigonometric representation may be used, and one form of the integral could be

$$\bar{C}_{N,m} = 2 \int_{x_2}^{\ell} \left\{ \left(\frac{p_b}{p_\infty} \right) \sum_{n=0}^{2} a_n \bar{\chi}_{x_2}^{n} - 1 \right\} \frac{2}{\gamma M_\infty^2} \sin \left(\frac{\pi}{2} \left(\frac{\ell - x}{\ell - x_2} \right) \right) \frac{x \tan \phi}{A_R} dx$$

This would no doubt give an order of magnitude for the force but any value computed must be suspect.

6./

6. Discussion

As discussed in Part I the coefficients of $\bar{\chi}$ should perhaps be multiplied by (M_∞/M_b) for the flat plate at incidence, otherwise the surface pressure will be underestimated. The form of the polynomial will then be

$$\frac{p}{p_b} = \sum_{n=0}^{2} a_n \left\{ \left(\frac{M_\infty}{M_b} \right) \bar{\chi} \right\}^n .$$

This is the form that we have used throughout in the numerical examples presented in this section. As regards the coefficients (a_n) used, we have chosen those of Hayes and Probstein[1], and of Bertram and Blackstock.[7]

Bertram and Blackstock, for example, have shown that the viscous-induced pressure on a flat plate in the weak-interaction region can be expressed in terms of $\bar{\chi}$ by the equation

$$\frac{p}{p_b} = 1 + f(\bar{\chi}, \gamma, T_w/T_o) + f^2(\bar{\chi}, \gamma, (T_w/T_o))$$

where

$$f\left(\bar{\chi}, \gamma, \frac{T_w}{T_o}\right) = \frac{\lambda}{\sqrt{1+\lambda}} \left[1 + \frac{\lambda}{2(1+\lambda)} \right],$$

$$\lambda = \frac{\gamma g \bar{\chi}}{2},$$

and $$g = 1{\cdot}7208 \frac{(\gamma - 1)}{2} \left(\frac{T_w}{T_o} + 0{\cdot}3859 \right)$$ for a Prandtl number of unity.

Computations using Bertram and Blackstock's equation have been carried out for the cold-wall case $(T_w/T_o \to 0)$. These data have been curve fitted and the coefficients for use in equation (1) are

a_0 0·98036743

a_1 0·10887103

a_2 0·00055225112

giving a good fit to the actual theoretical values for the range $0 \leq \bar{\chi} \leq 20$.

Similarly,/

Similarly, for the <u>insulated-wall</u> case $(T_w/T_o \to 1)$, the coefficients are

$$a_o \quad 0{\cdot}95391181$$

$$a_1 \quad 0{\cdot}42157154$$

$$a_2 \quad 0{\cdot}0018173574$$

and the range of applicability of this fit is $0 \leqslant \bar{\chi} \leqslant 10$.

The upper limit in the insulated-wall case was determined so that $\bar{\chi}$ would be well in excess of the crossover value (from weak to strong interaction), which Bertram and Blackstock identify as occurring when the induced pressure becomes greater than four times the value for inviscid flow. For the insulated wall this occurs for $\bar{\chi} \geqslant 7$. For the cold-wall condition the induced pressure does not exceed four times the inviscid pressure until a value of $\bar{\chi}$ is reached which is well within the merged region, and this suggests, as we observed in the first section (Part I), that there will be no strong-interaction region.

The insulated-wall pressure distribution for the strong-interaction region computed from Bertram and Blackstock's paper is given by

$$\frac{p}{p_b} \approx 1 + 0{\cdot}510036\,\bar{\chi}$$

The total normal forces on the lower or pressure surface of the delta computed using the various first- and second-order theories are shown in Fig. 8. In this figure the term $0(1)$ denotes that first-order theory has been used for both the weak- and the strong-interaction regions, and $0(2) + 0(1)$ means that second-order theory has been used for the weak-interaction region and first-order theory for the strong-interaction region.

Note that both the second-order weak-interaction theories result in insulated-wall normal forces which are in agreement and lie significantly above the first-order, weak-interaction data. To a slightly smaller extent this also applies to the data using viscous-interaction data quoted by Cox and Crabtree[6]. As regards the variations of $\bar{\chi}$ with incidence, it is the increase in Reynolds number and decrease in Mach number over the surface of the delta with increasing incidence up to about 15°, and thereafter mainly the decreasing Mach number, which produces a steady decrease in $\bar{\chi}$. In fact because the Reynolds number is only raised to the power 0·5 whereas the Mach number is raised to power 3 it is the Mach number of course which plays the important role in viscous-interaction effects, when the change in Reynolds number is moderate. It is most important that this be borne in mind when determining the operational range of hypersonic facilities.

7./

7. Conclusions

As a result of the induced pressures produced by the interaction of the viscous layer with the continuum flow, significant changes will occur in the normal-force coefficient for the pressure surface of a flat delta at the moderate Reynolds numbers and hypersonic Mach numbers frequently encountered in test facilities. It is felt that the present approach enables a reasonable estimate to be made of the possible changes in viscous-induced force and moment characteristics, at least for simple planforms and surface shapes.

References/

References

No.	Author(s)	Title, etc.
1	W. D. Hayes and R. F. Probstein	Hypersonic flow theory. Academic Press. 1959.
2	S. C. Metcalf, D. C. Lillicrap and C. J. Berry	A study of the effects of surface condition on the shock-layer development over sharp-edged shapes in low Reynolds number high speed flow. Paper given at the 6th Int. Symp. on Rarefied Gas Dynamics, Boston. 1968.
3	J. C. Cooke	Leading edge effects on caret wings. ARC CP 0978. 1964.
4	E. S. Moulic and G. J. Maslach	Induced pressure measurements on a sharp edged insulated flat plate in low density hypersonic flow. 5th Rarefied Gas Dynamics Symposium, Vol.II, Oxford. 1966. Academic Press. pp
5	S. C. Metcalf	Private communication.
6	R. N. Cox and L. F. Crabtree	Elements of hypersonic aerodynamics. The English Universities Press Ltd. 1965.
7	M. H. Bertram and T. A. Blackstock	Some simple solutions to the problem of predicting boundary-layer self-induced pressures. NASA TN D-798. 1961.

BMG

32117
FIG. 1

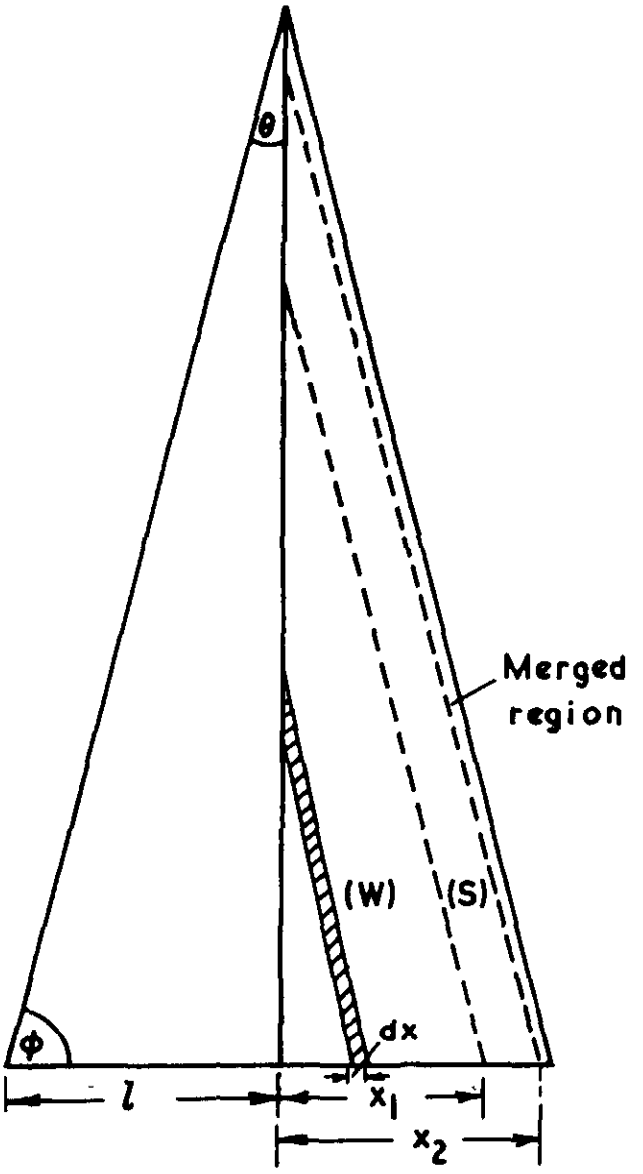

Indicating weak (W) interaction region and strong (S) interaction region

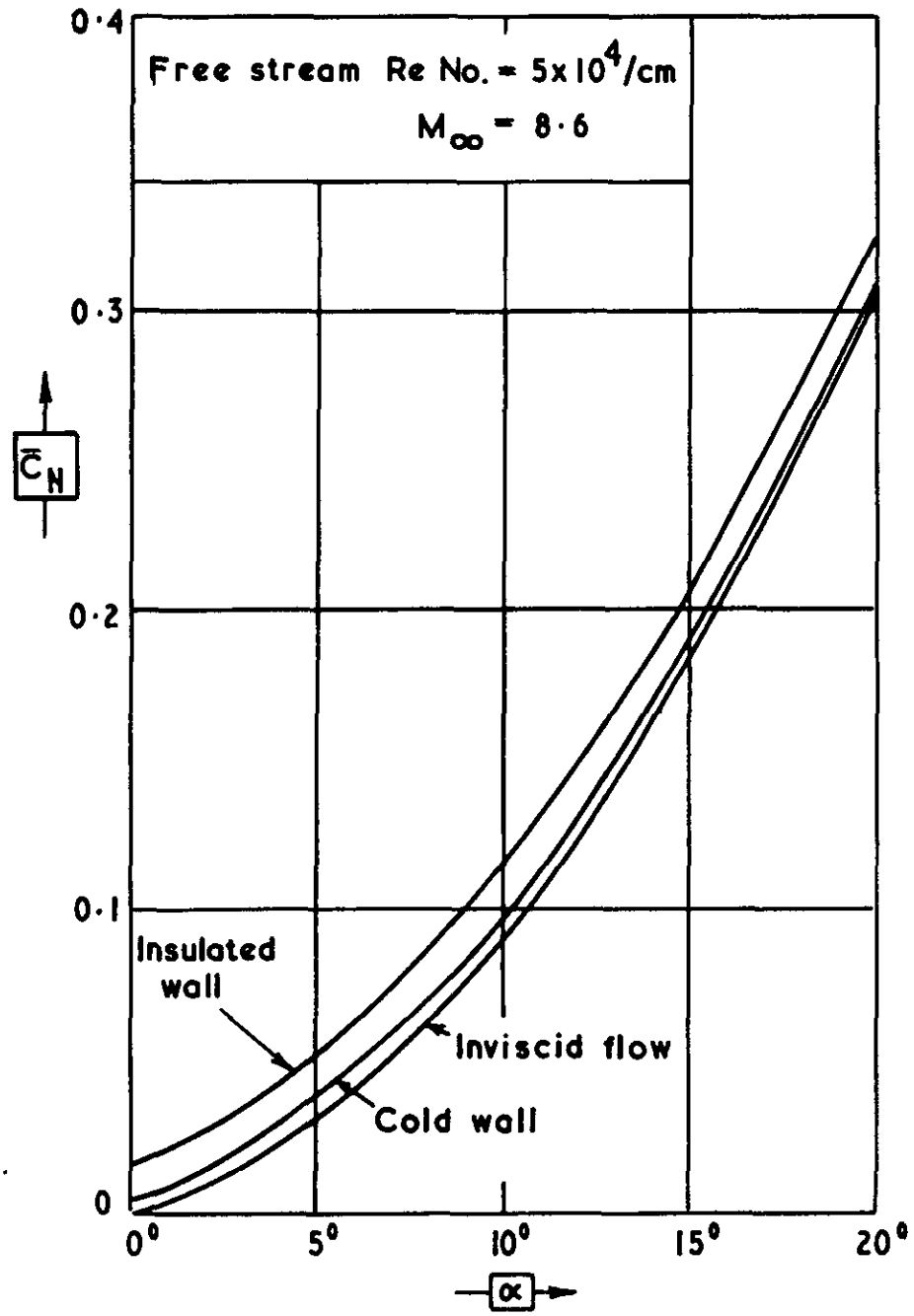

Lower surface

Normal-force coefficient as a function of incidence (delta wing, $\phi = 76^0$)

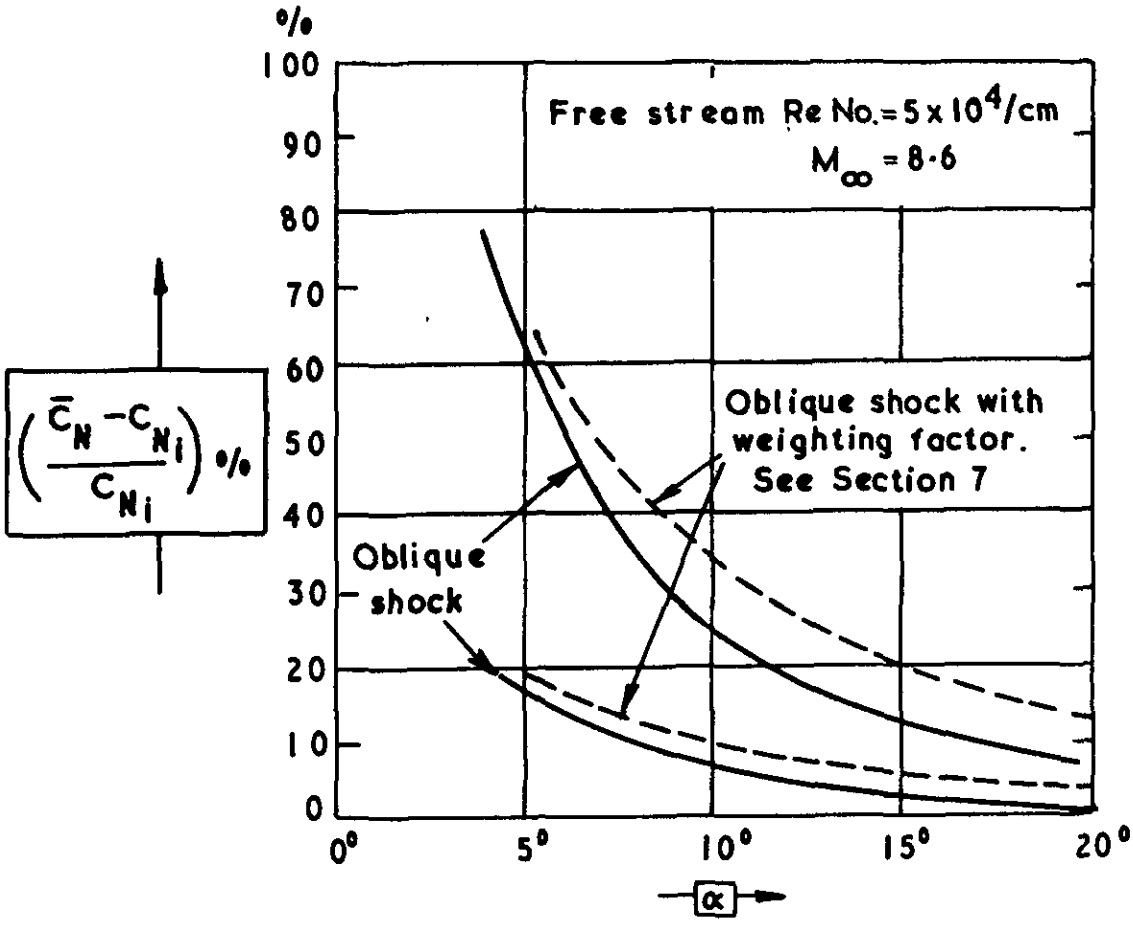

Lower surface

Percentage increase in inviscid-flow normal force as a function of incidence (delta wing, $\phi = 76^0$)

32117

FIG.4

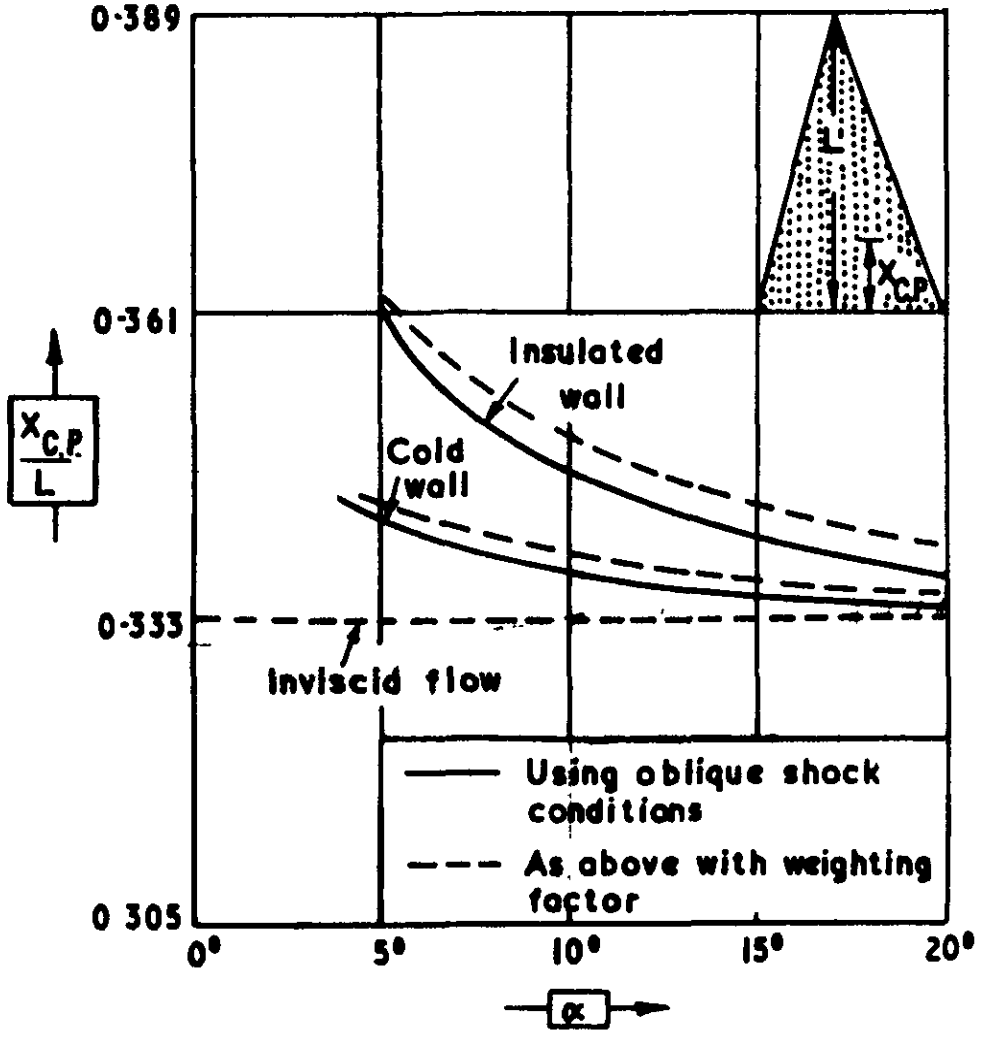

Lower surface

Distance of centre of pressure from base line divided by centre chord length $\left(\frac{X_{C.P.}}{L}\right)$ as a function of incidence (α)

(delta wing, $\phi = 76^{\circ}$)

32117
FIG.5

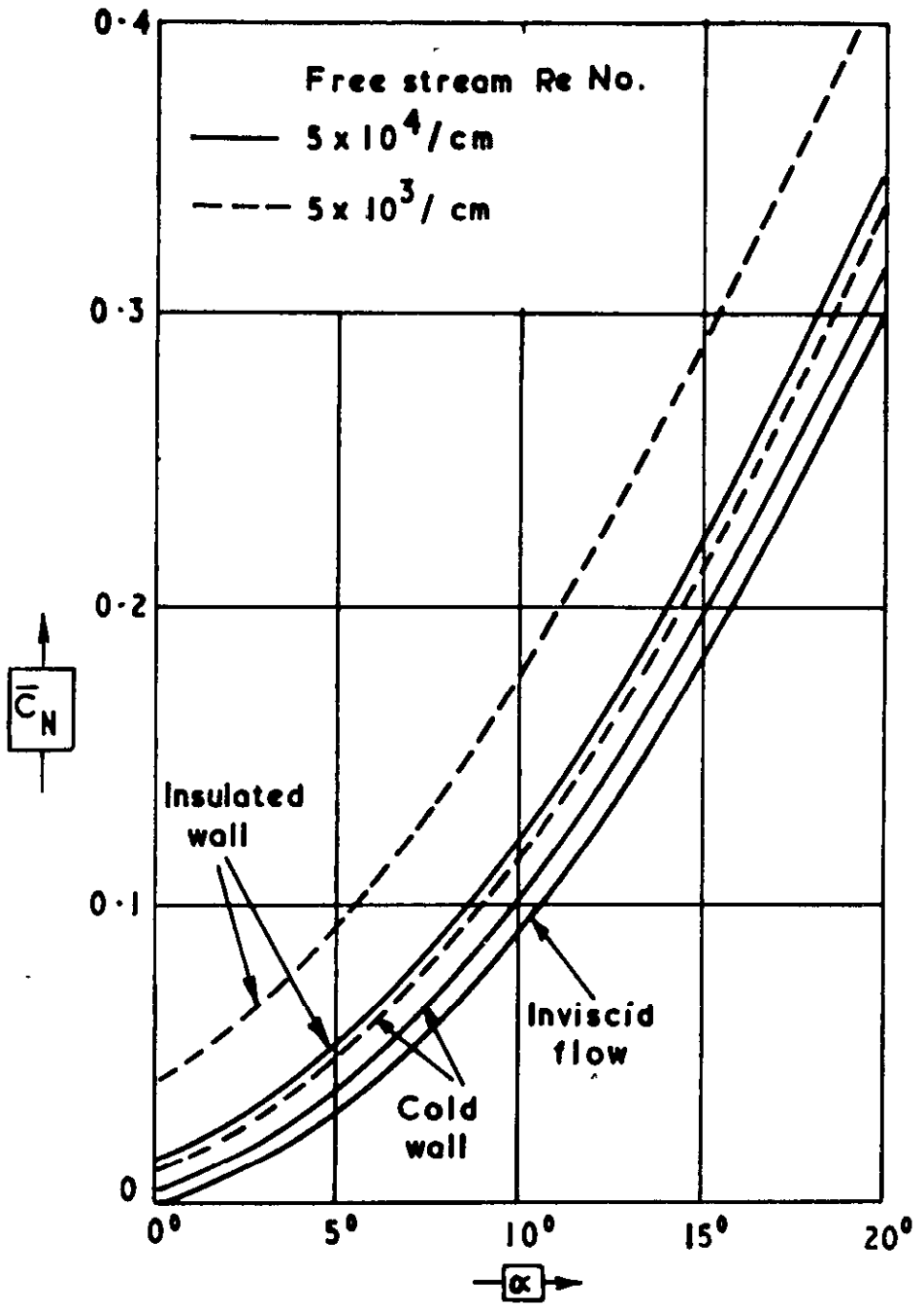

Lower surface

Total normal-force coefficient versus incidence(delta wing, $\phi = 76^0$)

32117
FIG. 6

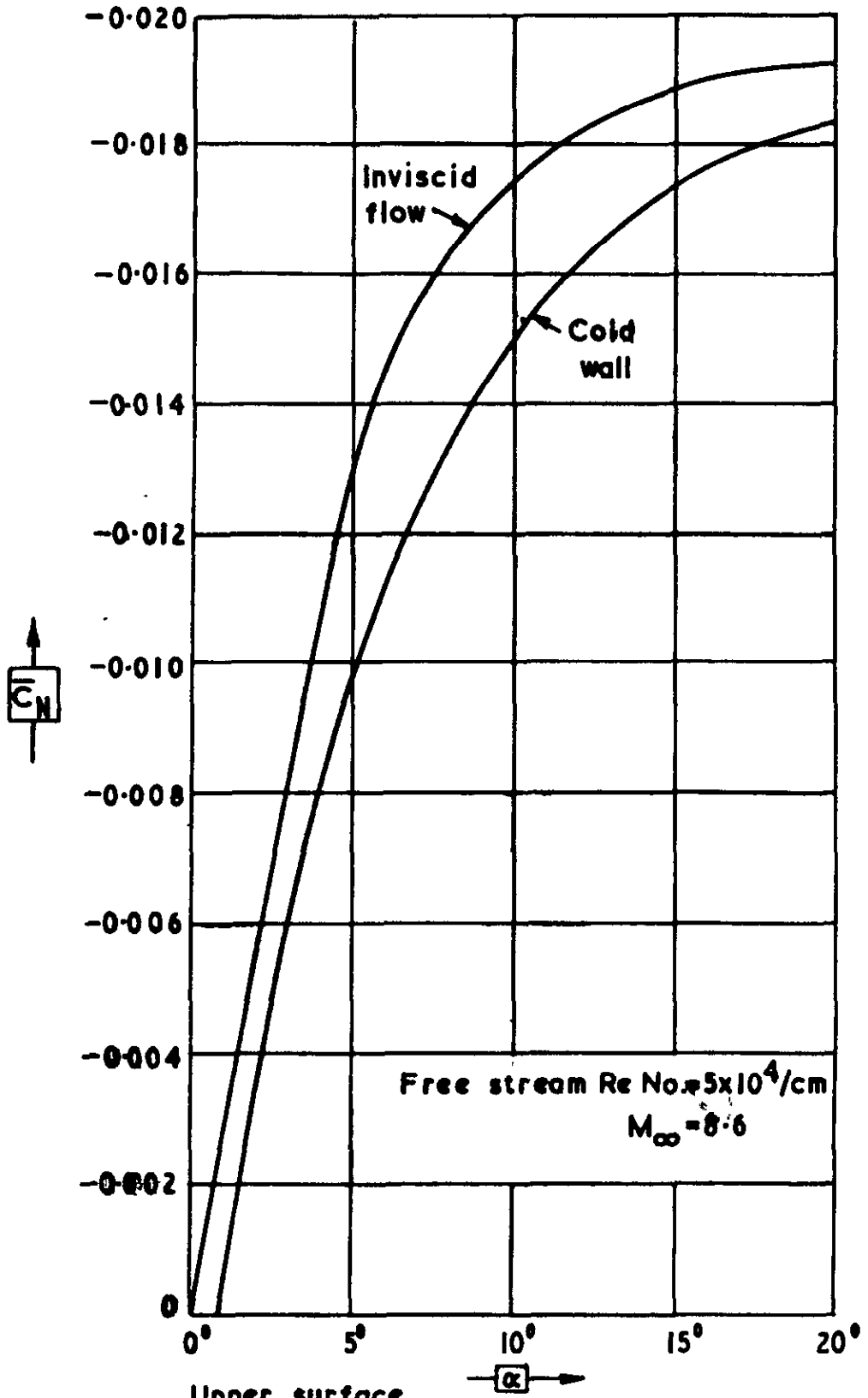

Upper surface

Total normal-force versus incidence for inviscid-flow and for cold-wall viscous conditions (delta wing, $\phi = 76^\circ$)

32117
FIG. 7

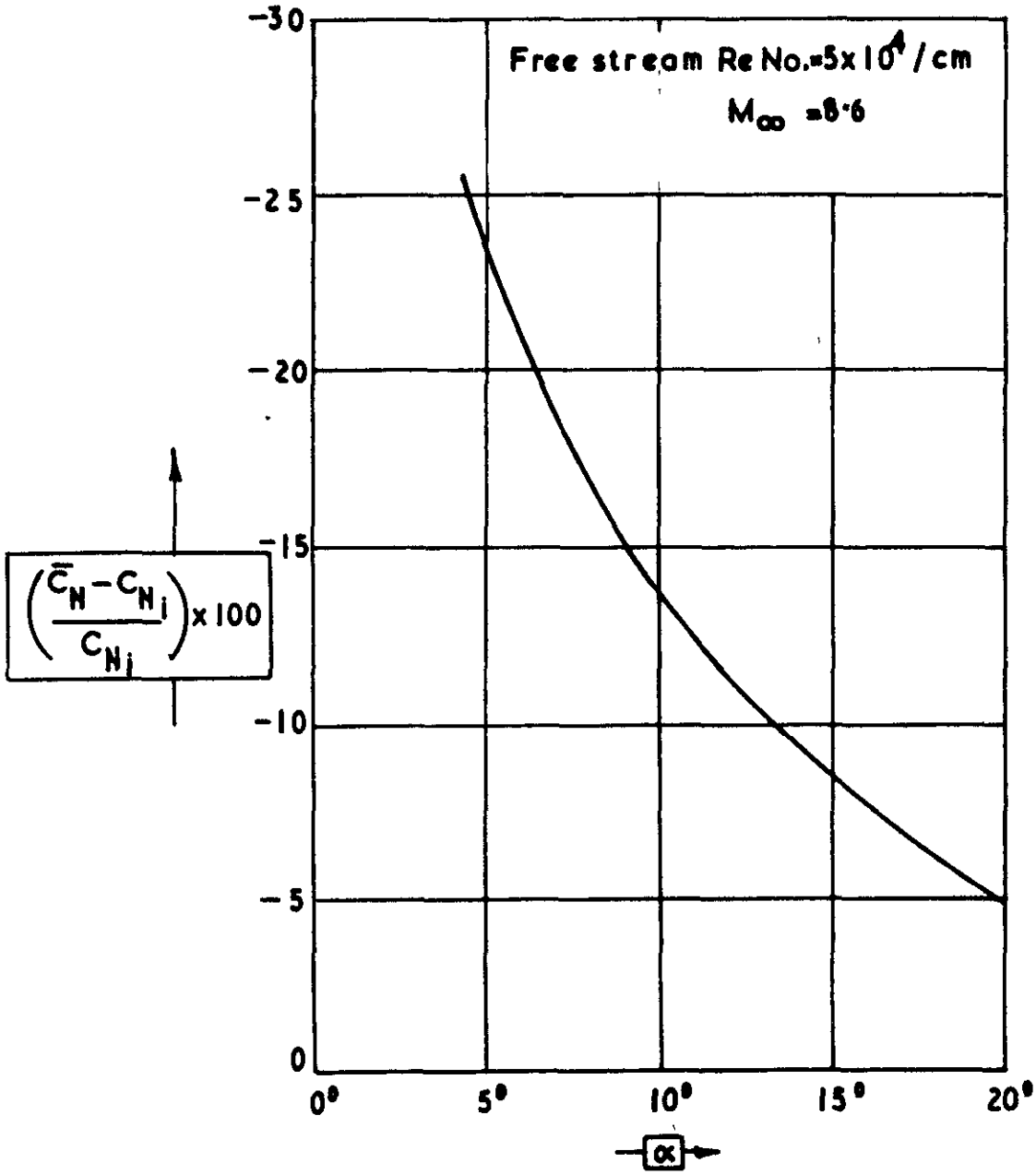

Upper surface

Percentage decrease in upper-surface force coefficient for cold wall conditions

(delta wing, $\phi = 76^\circ$)

32117

FIG.8

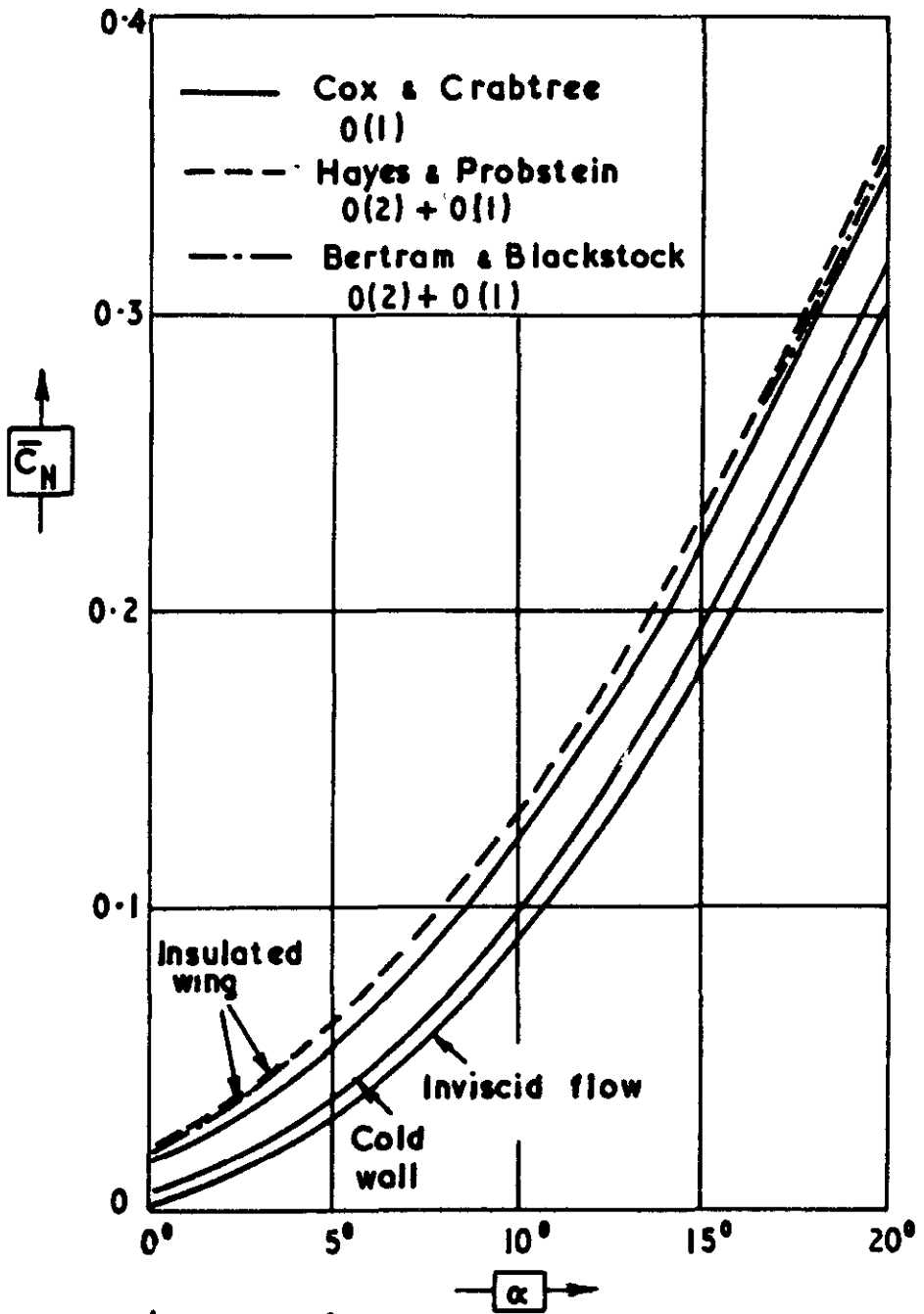

Lower surface

Total normal-force coefficient versus incidence using various theories. Free stream Re No. = 5×10^4/cm

R 15080/1/S02109 K4 1/73 P

ARC CP No. 1237
May, 1970

Davies, L.

ON THE EFFECTS OF VISCOUS INTERACTION FOR A FLAT DELTA WING AT INCIDENCE

Equations are derived which enable the effects of viscous interaction on the normal force to be assessed for a flat delta wing at incidence.

ARC CP No. 1237
May, 1970

Davies, L.

ON THE EFFECTS OF VISCOUS INTERACTION FOR A FLAT DELTA WING AT INCIDENCE

Equations are derived which enable the effects of viscous interaction on the normal force to be assessed for a flat delta wing at incidence.

ARC CP No. 1237
May, 1970

Davies, L.

ON THE EFFECTS OF VISCOUS INTERACTION FOR A FLAT DELTA WING AT INCIDENCE

Equations are derived which enable the effects of viscous interaction on the normal force to be assessed for a flat delta wing at incidence.

HER MAJESTY'S STATIONERY OFFICE

Government Bookshops

49 High Holborn, London WC1V 6HB
13a Castle Street, Edinburgh EH2 3AR
109 St Mary Street, Cardiff CF1 1JW
Brazennose Street, Manchester M60 8AS
50 Fairfax Street, Bristol BS1 3DE
258 Broad Street, Birmingham B1 2HE
80 Chichester Street, Belfast BT1 4JY

Government publications are also available through booksellers

C.P. No. 1237

SBN 11 470795 2